# Axitinib Improves Radiotherapy in Murine Xenograft Lung Tumors

Gilda G. Hillman*, Fulvio Lonardo[†],
David J. Hoogstra*, Joseph Rakowski*,
Christopher K. Yunker*, Michael C. Joiner*,
Gregory Dyson[‡,§], Shirish Gadgeel[§]
and Vinita Singh-Gupta*

*Department of Radiation Oncology, Barbara Ann Karmanos
Cancer Institute, Wayne State University School of
Medicine, Detroit, MI 48201, USA; [†]Department of
Pathology, Barbara Ann Karmanos Cancer Institute, Wayne
State University School of Medicine, Detroit, MI 48201,
USA; [‡]Department of Biostatistics Core, Barbara Ann
Karmanos Cancer Institute, Wayne State University School
of Medicine, Detroit, MI 48201, USA; [§]Department of
Oncology, Barbara Ann Karmanos Cancer Institute, Wayne
State University School of Medicine, Detroit, MI 48201, USA

## Abstract

A third of patients with non-small cell lung cancer (NSCLC) present with un-resectable stage III locally advanced disease and are currently treated by chemo-radiotherapy but the median survival is only about 21 months. Using an orthotopic xenograft model of lung carcinoma, we have investigated the combination of radiotherapy with the anti-angiogenic drug axitinib (AG-013736, Pfizer), which is a small molecule receptor tyrosine kinase inhibitor that selectively targets the signal transduction induced by VEGF binding to VEGFR receptors. We have tested the combination of axitinib with radiotherapy in nude mice bearing human NSCLC A549 lung tumors. The therapy effect was quantitatively evaluated in lung tumor nodules. The modulation of radiation-induced pneumonitis, vascular damage and fibrosis by axitinib was assessed in lung tissue. Lung irradiation combined with long-term axitinib treatment was safe resulting in minimal weight loss and no vascular injury in heart, liver and kidney tissues. A significant decrease in the size of lung tumor nodules was observed with either axitinib or radiation, associated with a decrease in Ki-67 staining and a heavy infiltration of inflammatory cells in tumor nodules. The lungs of mice treated with radiation and axitinib showed a complete response with no detectable residual tumor nodules. A decrease in pneumonitis, vascular damage and fibrosis were observed in lung tissues from mice treated with radiation and axitinib. Our studies suggest that axitinib is a potent and safe drug to use in conjunction with radiotherapy for lung cancer that could also act as a radioprotector for lung tissue by reducing pneumonitis and fibrosis.

*Translational Oncology (2014) 7, 400–409*

## Introduction

Lung cancer is the second most common malignancy in both men and women in the USA and the leading cause of death. It is estimated that over 215,000 people per year will be diagnosed with lung cancer [1]. Approximately 85% of lung cancers are classified as non-small cell lung cancer (NSCLC), which includes squamous cell carcinoma, adenocarcinoma and large cell carcinoma. A third of patients with newly diagnosed NSCLC present with unresectable stage IIIA or stage

http://dx.doi.org/10.1016/j.tranon.2014.04.002

IIIB locally advanced disease with an overall 5-year survival rate of 16% [2]. Locally advanced disease is currently treated by chemo-radiotherapy [3–5]. Several trials showed that concurrent cisplatin chemotherapy with radiotherapy (RT) is superior to sequential chemotherapy followed by RT or to RT alone; however the median survival is only about 21 months [4]. Biological agents are currently being tested to improve the outcome of chemo-RT for locally advanced NSCLC including anti-angiogenic drugs and cetuximab, an anti-EGFR antibody (Ab) [6]. Bevacizumab, an anti-VEGF monoclonal Ab that acts as an anti-angiogenic drug, showed modest benefit when used in combination with first line carboplatin-paclitaxel or cisplatin and gemcitabine chemotherapy in patients with non-squamous advanced NSCLC [7,8]. Because bevacizumab has a prolonged half-life, which allows administration every 2-3 weeks, toxicity and bleeding are of concern [7]. Bevacizumab significantly increased the risk of grade ≥3 proteinuria, hypertension, haemor-rhagic events, neutropenia and febrile neutropenia compared to chemotherapy alone [9]. Bevacizumab given with concurrent thoracic radiotherapy for stage III NSCLC also resulted in severe pneumonitis in a recent phase I clinical trial [10] and increased esophagitis in other trials with radiotherapy [11,12]. Novel anti-angiogenic drugs with shorter half-life than bevacizumab, and that could be less toxic, include small molecule receptor tyrosine kinase (RTKs) inhibitors target VEGF receptors (VEGFR) and inhibit the signal transduction induced by VEGF binding to VEGFR. These drugs are administered daily because of their short-half-life [13]. Among others, sunitinib, a multiple RTK inhibitor, has shown efficacy in metastatic renal cell carcinoma but has dose-limiting toxicity [13]. Sunitinib had limited efficacy in NSCLC and is currently tested in clinical trials in combination with chemotherapy [14,15]. Axitinib (AG-013736, Pfizer) is a more selective RTK inhibitor of all three VEGF receptors VEGFR-1, -2 and -3 than sunitinib [16]. Axitinib has a high potency for VEGFR-2, the main receptor involved in VEGF binding that is critical for induction of angiogenesis and therefore could target the tumor sites more specifically [16,17]. Axitinib has proven to be a very potent inhibitor of VEGFR-2 signaling in pre-clinical studies [18–21]. Advantages of axitinib over other anti-angiogenic drugs are that it has a favorable profile of toxicity with the absence of cumulative dose-limiting toxicity and it can be given in a constant and manageable schedule of administration [16]. This drug has a shorter half-life (2-5 h) than bevacizumab and its daily administration could be better controlled to limit toxicity [22]. Axitinib used in a phase II trial for advanced NSCLC demonstrated an increased one-year survival rate with manageable toxicities [17,22] and was well tolerated when combined with platinum doublets chemotherapy [23]. The role of angiogenesis in the progression and prognosis of NSCLC and its targeting by various new anti-angiogenic drugs either alone or combined with conventional chemotherapy for NSCLC are under extensive clinical investigation [24–27]. However, the combination of anti-angiogenic drugs with RT, which is the conventional treatment for stage III inoperable NSCLC, has not been explored.

The goal of the current study was to explore whether axitinib could improve the efficacy of RT for NSCLC using a pre-clinical model of orthotopic lung carcinoma. We hypothesized that an anti-angiogenic drug, given at doses which trim inefficient tumor vessels and regularize blood flow, could improve oxygenation in the tumor microenvironment and enhance RT efficacy for locally advanced NSCLC. Alternatively, higher doses of anti-angiogenic drugs resulting in a cytostatic effect could enhance the cytoreductive effect of RT. Using these concepts, we have previously demonstrated that a dose of sunitinib, which regularized tumor vessels and blood flow, enhanced the efficacy of chemo- and radio-therapies for metastatic RCC in an orthotopic RCC pre-clinical mode [28–30]. However, the dose of sunitinib used in these studies was reduced to avoid toxicity to the vasculature of normal tissues [28–30]. We now report studies confirming that axitinib is a potent and safe anti-angiogenic drug that significantly enhances the efficacy of lung irradiation in an orthotopic xenograft model of lung carcinoma. This combined therapy is well tolerated with no further increase in radiation-induced injury or vascular damage in lung tissue but quite the opposite effect was observed suggesting a radioprotective effect.

## Materials and Methods

### Establishment of NSCLC Lung Tumor Model

The human non-small cell lung carcinoma (NSCLC) A549 (purchased from ATCC) was cultured in F-12 K culture medium containing 7% heat-inactivated fetal bovine serum with supplements. A549 cells, at $2 \times 10$ [6] in 200 μl HBSS, were injected i.v. in the tail vein of 5-6 week old female Hsd Athymic Nude-Foxn1$^{nu}$ *nu/nu* nude mice (Harlan, Indianapolis, IN) [31]. Mice were housed and handled under sterile conditions in facilities accredited by the American Association for the Accreditation of Laboratory Animal Care (AAALAC). The animal protocol was approved by Wayne State University Animal Investigation Committee (IACUC).

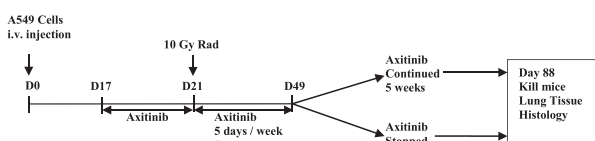### Tumor-bearing lung irradiation

Three anesthetized mice, in jigs, were positioned under a 6.4 mm lead shield with 3 cut-outs in an aluminum frame mounted on the X-ray machine to permit selective irradiation of tumor-bearing lungs in the thoracic area, as previously described [31]. The radiation dose to the lung and the scattered dose to areas of the mouse outside of the radiation field were carefully monitored. Photon irradiation was performed at a dose of 10 Gy with a Siemens Stabilipan X-ray set (Siemens Medical Systems, Inc) operated at 250 kV, 15 mA with 1 mm copper filtration at a distance of 47.5 cm from the target. A high dose of radiation of 10 Gy was selected for these studies with the rationale that such a dose could inflict greater damage to normal lung tissue and will allow for evaluation of potential injury aggravation by axitinib.

### Experimental protocol

Axitinib (Pfizer Inc, New York, NY), was prepared in a carboxymethyl cellulose suspension vehicle, and given orally by gavage at a dose of 25 mg/kg (0.5 mg/mouse) per day, once a day. The dose was selected to give an intermediate effect for combination with radiation, based on previous titration studies [20]. As previously reported, to monitor tumor establishment in the lungs of mice, preliminary kinetics experiments were performed and mice were sacrificed at different time points after i.v. injection of A549 cells [31,32]. Lungs were resected and processed for histological staining with hematoxylin-eosin (H&E). Established tumor nodules of about 100-300 μm in diameter were detected by day 17-18 in the midst of the lung tissue, therefore this time point was selected to initiate treatment with axitinib. Tumor bearing mice were pre-treated with axitinib for 4 days from day 17-20 (Table 1A). Then, on day 21, the full lung was selectively irradiated by delivering 10 Gy to the thorax while shielding the rest of the mouse body with lead. Axitinib treatment was resumed at 25 mg/kg/day and given 5 days a week for 5 more weeks (Table 1A). At this time point, axitinib was

**Table 1.** Axitinib combined with radiation in mice-bearing A549 lung tumors.

A. Treatment Schedule

```
A549 Cells              10 Gy Rad
i.v. injection             |                        Axitinib
     |                     |                        Continued        Day 88
     ↓                     ↓                        5 weeks          Kill mice
     D0    D17    D21           D49          →                   →  Lung Tissue
              Axitinib                                              Histology
                    Axitinib               Axitinib
                    5 days / week          Stopped
                    for 5 weeks
```

B. Effect of therapy on mouse weight

Mouse weight (mean ± SE in gm)

| Treatment | Day 25 | Day 36 | Day 46 | Day 53 | Day 67 | Day 79 |
|---|---|---|---|---|---|---|
| Control | 23.1 ± 0.4 | 24.0 ± 0.4 | 24.7 ± 0.4 | 24.3 ± 0.5 | 25.4 ± 0.6 | 26.6 ± 0.7 |
| Axitinib (10 Weeks) | 22.0 ± 0.5 | 22.3 ± 0.5 | 23.2 ± 0.6 | 22.4 ± 0.9 | 23.8 ± 0.9 | 24.7 ± 1.1 |
| Axitinib (5 weeks) | N/A | N/A | N/A | 23.4 ± 0.5 | 23.7 ± 0.9 | 25.5 ± 1.0 |
| Rad | 21.4 ± 0.3 | 22.4 ± 0.7 | 23.3 ± 0.3 | 24.2 ± 0.3 | 25.1 ± 0.3 | 24.7 ± 0.8 |
| Rad + Axitinib (10 weeks) | 21.9 ± 0.7 | 23.0 ± 0.6 | 23.5 ± 0.6 | 22.6 ± 1.0 | 23.4 ± 1.2 | 24.3 ± 1.4 |
| Rad + Axitinib (5 weeks) | N/A | N/A | N/A | 24.4 ± 0.6 | 25.3 ± 0.8 | 26.5 ± 0.7 |

A. Treatment schedule: Mice bearing A549 lung tumors were pre-treated with axitinib at 25 mg/kg/day for 4 days, on days 17-20 after i.v. A549 cell injection. Then, mice received 10 Gy radiation to the tumor-bearing lungs on day 21. Axitinib was continued 5 days a week for up to 5 weeks (day 49). In treatment groups of mice receiving axitinib alone or axitinib + radiation, axitinib was discontinued in half of the mice whereas the other half of the mice received 5 more weeks of axitinib. Mice were monitored for about 3 months and killed on day 88.

B. Mouse weight: Mice bearing A549 lung nodules treated with Axitinib for 4 days then with 10 Gy radiation to the whole lung. After radiation, axitinib was given for 10 weeks or was discontinued after 5 weeks.

discontinued in half of the mice whereas the other half of the mice received 5 more weeks of axitinib. The number of mice per treatment group was 8 in control, 8 in axitinib, 9 in radiation and 9 in radiation + axitinib. To assess the therapeutic response of lung tumors to axitinib and radiation, mouse survival was monitored in a long-term experiment of about 3 months. Mice exhibiting weight loss, lethargy or gross metastases in the limbs were killed and lungs were perfused with 10% buffered formalin prior to resection.

## Histology of lung tissue sections

Formalin fixed lungs were embedded in paraffin and sectioned into 5 μm sections. Sections were stained with (H&E). Quantitation of histological findings was performed by evaluation of lung tissues using a Nikon E-800 microscope. The number of nodules in the five lobes of the mouse lungs was enumerated. Morphometric measurements of each tumor nodule were performed using Image-ProPlus version 6.2 software (MediaCybernetics) [31]. The two largest diameters of each nodule were measured and computed to estimate the nodule surface area. The same software was used to measure the thickness of alveolar septa on H&E slides as an estimate of pneumonitis. The ratio of alveolar septa area relative to the total area of a 20X field was quantified while contouring and excluding bronchioles and large vessels (see inset Table 3) and was performed in 20 fields of 20X, as previously published [33]. Proliferation of tumor cells in lung nodules was assessed by Ki-67 nuclear staining with anti-Ki-67 antibody (Ab) (LifeSpan, Seattle, WA) followed by anti-rabbit biotinylated secondary Ab (Vector Laboratories, Burlingame, CA); using an avidin-biotin immunoperoxidase technique (Vector). The extent of fibrosis was evaluated using Masson's Trichrome stain (NovaUltra Kit, IHCWORLD, Woodstock, MD) [31,33]. The lung vasculature was visualized by fluorescent immunostaining, as previously shown in

other studies [34–36]. Endothelial cells were identified with rat anti-mouse CD31 Ab (Thermo Scientific, Fremont, CA) followed by tetramethylrhodamine (TRITC)-labeled secondary goat anti-rat Ab (Molecular Probes, Grand Island, NY). Pericytes were identified with mouse anti-α-SMA (Sigma, St. Louis, MO) followed by Alexa Fluor 350-conjugated secondary goat anti-mouse Ab. The vessel basement membrane was stained with rabbit anti-collagen type IV Ab (Millipore, Billerica, MA) followed by Alexa Fluor 488-conjugated secondary goat anti-rabbit Ab (Molecular Probes). All slides were examined using a Nikon E-800 fluorescent microscope. Digital images were taken separately with each fluorescent dye, including red for endothelial cells, blue for pericytes and green for collagen, and were then processed to create composite images with the three colors using Image-ProPlus version 6.2 software.

### Statistical analysis

Differences in mouse weight among the various treatments groups were analyzed by two-tailed unpaired Student's t-test. For histological data analysis, differences in the number and size of tumor nodules, and Ki-67 positive tumor nuclei among the various treatments groups were analyzed by two-tailed unpaired Student's t-test [31]. The Fisher's Exact test was used to assess the differences in proportion of damaged vessels between treatment groups. No adjustments for multiple testing were done. A p-value of 0.05 was considered statistically significant.

## Results

### Treatment of A549 lung tumor nodules with axitinib and radiation: Safety of long-term treatment

To assess the long-term effect of axitinib combined with lung irradiation, mice bearing established A549 lung tumor nodules were treated with each modality or both combined as depicted in the schedule presented in Table 1A. The need for prolonged axitinib treatment after radiation and its safety were addressed by either stopping axitinib after 5 weeks or continuing for 5 more weeks (Table 1A). To assess the safety of the long-term treatment, mice were weighed at various time points during the experiment, on days 25, 36, 46, 53, 67 and 79 (Table 1B). Compared to control untreated mice, a mild decrease in mouse weight was observed following treatment with radiation, axitinib and both combined of about 3-8% (Table 1B). However, mice continued to gain weight in all treatment groups. No statistical differences were obtained when the weight of treatment groups were compared to control group or combined therapy was compared to single modality (p > 0.1), suggesting a non-significant minimal overall effect on the mouse weight. A mild increase in weight was observed after axitinib was discontinued in axitinib treated mice and radiation + axitinib treated mice. No obvious signs of toxicity and no skin rashes indicative of bleeding were observed in mice treated with radiation and axitinib, these mice were normally active during the duration of the 3 months experiment. Histological analysis of tissues from kidneys, heart and liver showed no alterations in the vasculature of these organs by systemic treatment with axitinib alone or combined with radiation, confirming the safety of the drug.

Mice were killed if they showed signs of distress including weight loss, lethargy and tumors in limbs, due to cancer spread. Two control mice with high lung tumor burden developed tumors in limbs and metastatic hilar lymph nodes by day 77. Overall survival in this experiment by day 88 was 50% for control mice, 100% for mice treated with axitinib for 10 weeks, 75% for mice treated with axitinib for 5 weeks, 88% in mice treated with radiation and 100% in mice
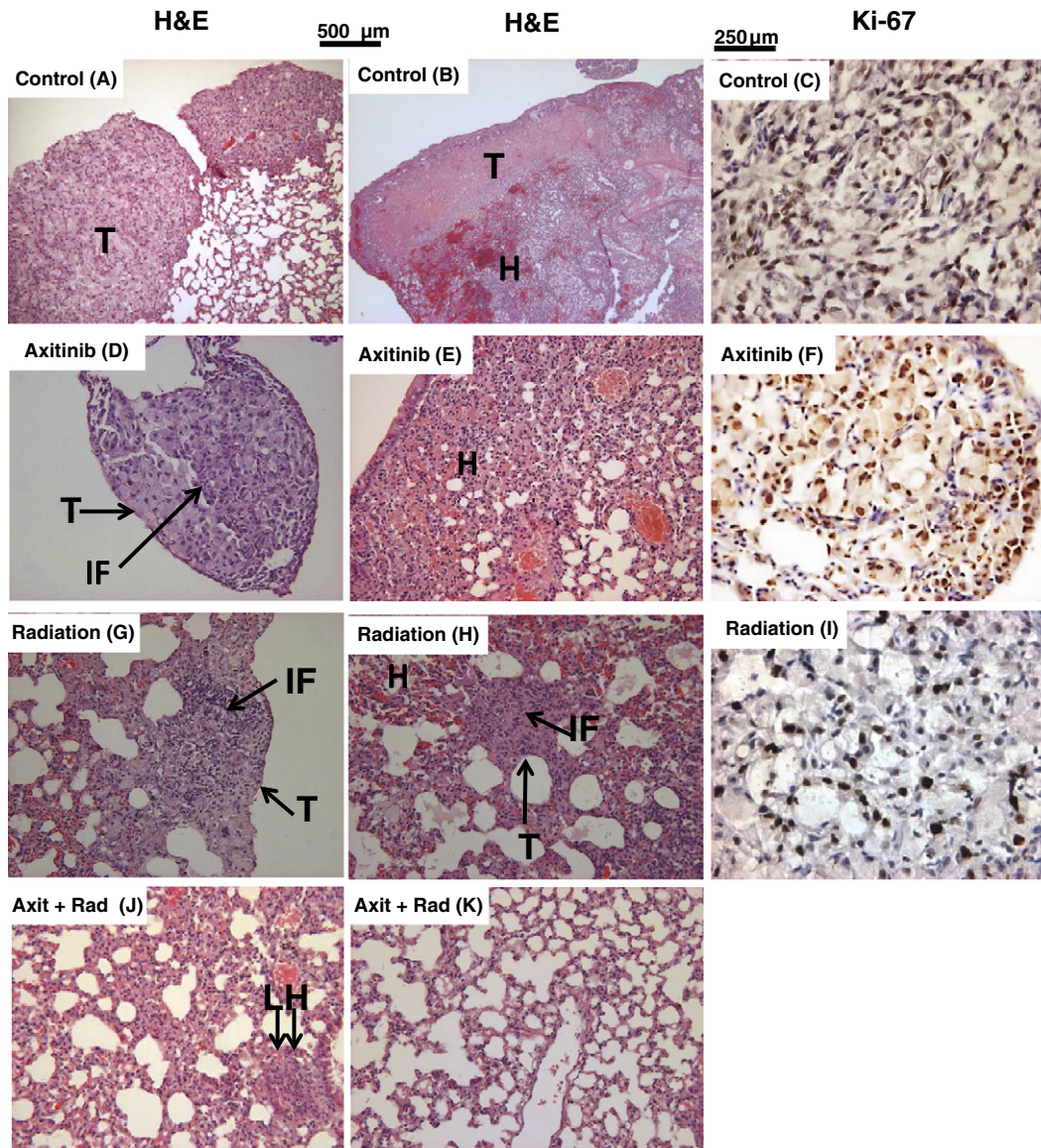
treated with axitinib and radiation. No statistical differences were obtained in the survival of mice at day 88 in the comparison of single modality treatment groups versus combined modality treatment groups (p = 0.72).

### Enhanced therapeutic response in lung tumor nodules by axitinib combined with high dose radiation

The therapeutic effect of axitinib and radiation of mice treated with the schedule described in Table 1A was assessed in lung tissue sections processed for H&E staining. In the control group, mice surviving up

to 70-88 days had very large tumor nodules, which histologically presented as large pleomorphic tumor cells with cytoplasmic vacuoles, large nuclei and prominent nucleoli (Figure 1A), compatible with poorly differentiated adenocarcinoma. Some of the large nodules were hemorrhagic and necrotic (Figure 1B). The number of measurable tumor nodules was estimated at 30-40 per lung, some were not countable as they coalesced replacing large lung areas (Table 2). A wide range of sizes was measured however most of them were very large, and hemorrhagic with a mean area of $110 \times 10^4$ $\mu m^2$ (Table 2). These tumors showed a high proliferation index by Ki-67 staining



**Figure 1.** H &E and Ki-67 staining of lung tissue sections from mice treated with axitinib and radiation. Lung tissue sections were processed for H& E staining and Ki-67 immunostaining. Lung sections from control mice showing large tumor nodules (T) and extensive hemorrhages (H) in the vicinity of invasive tumor nodules (panels A and B) with a high Ki-67 proliferation index in tumor nodules (panel C). Following axitinib treatment, smaller tumor nodules with decreased cellularity and chronic inflammatory infiltrates (IF) were seen (panel D) with focal areas of hemorrhages in lung tissue (panel E). Ki-67 staining showed decreased proliferation in tumor nodules (panel F). Radiation also resulted in small tumor nodules with decreased cellularity and heavy infiltration by chronic inflammatory cells (IF) (panel G, H). Focal areas of hemorrhages and enlarged septa in lung tissue were observed (panel H). Ki-67 staining showed decreased proliferation in tumor nodules (panel I). Following axitinib combined with radiation, no tumor nodules were detectable but only isolated lymphohistiocytic nodules (LH, see arrows in panel J). Large areas of normal lung parenchyma were seen (panel K). Magnifications are 20x (bar size of 500 $\mu m$) for all H & E pictures (A,B,D,E,G,H,J,K) to emphasize the effect of therapy both in tumor nodules and in lung tissue. Magnifications are 40x (bar size of 250 $\mu m$) for all Ki-67 pictures (C,F,I) to show nuclei staining in the tumor cells.

**Table 2.** Quantitation and morphometric measurements of A549 lung tumor nodules from mice treated with axitinib and radiation.

| | # Tumor Nodules[a] | Nodule Area[b] mean ± SE×10$^4$ μm$^2$ | Range[c] (x10$^4$μm$^2$) | Ki-67+ Nuclei[d] mean ± SE | Fibrosis[e] |
|---|---|---|---|---|---|
| Control | 30[&] | 110 ± 24 | 13 – 503 | 111 ± 10.4 | ± |
| Axitinib | 21 | 10 ± 3 | 0.8 – 50 | 40 ± 1 | ± |
| Radiation | 34 | 8.4 ± 1.9 | 1.2 – 43 | 42 ± 9.7 | + + + |
| Rad + Axit (10w) | 0 | 0 | 0 | 0 | ± |
| Rad + Axit (5w) | 0 | 0 | 0 | 0 | ± |

[a] In H&E stained lung tissue sections, the tumor nodules were enumerated from 2 mice per treatment group.[&]In control group, we are reporting 30 representative measurable tumors as some of the nodules were invading large areas of septae and were not measurable. In the last treatment groups, axitinib was continued for 10 weeks [Rad + Axit (10w)] or discontinued after 5 weeks [Rad + Axit (5w)].

[b] The nodule area was estimated by morphometric measurements of each tumor nodule and the mean ± SE of all nodules is reported.

[c] The range of nodule area is presented.

[d] The number of Ki-67 positive nuclei in tumor cells was enumerated in tumor nodules. The mean positive nuclei per tumor nodule ± SE is reported.

[e] The extent of fibrosis was scaled from weak (±) to heavy (+ + +).
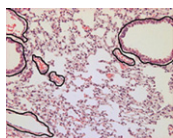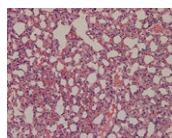
with an average of about 110 positive nuclei per nodule (Figure 1C). The lung tissue showed a mix of normal lung alveoli and focal areas of thick alveolar septa with hemorrhages which were observed in the vicinity of tumor nodules (Figure 1B). Following treatment with axitinib, several tumor nodules were still observed in the lung (Figure 1D, Table 2), but these nodules were significantly smaller than in control mice with a mean area of $10 \times 10^4$ μm$^2$ (p = 0.001, Table 2) and contained chronic inflammatory infiltrates (Figure 1D). Focal areas of hemorrhages were observed in the lung tissue (Figure 1E). A decrease in both cellularity and proliferative nuclei were observed in the tumor nodules with a mean of Ki-67 positive nuclei of 40 (Figure 1 F, Table 2, p < 0.01). Following radiation, numerous tumor nodules were observed with a wide range in size, however these nodules were significantly smaller than in control mice with a mean area of $8.4 \times 10^4$ μm$^2$ (p < 0.001, Table 2). Nodules showed alterations in tumor cells and inflammatory infiltrates (Figure 1G,H). Focal enlarged septa filled with chronic inflammatory cells were seen, which may represent foci of tumor destruction (Figure 1H). Akin to the effect of axitinib, radiation also caused a decrease in cellularity and dividing nuclei in tumors with a mean of Ki-67 positive nuclei of about 42 (Figure 1I, Table 2, p < 0.01). In

contrast, no tumor nodules were detectable in lungs treated with radiation and 10 weeks of axitinib but occasionally we observed distinctive lymphohistiocytic nodules consisting of lymphocytes and histiocytes with no detectable viable tumor cells (Figure 1 J; see arrows). These nodules probably represent an anti-tumor inflammatory response mediated by radiation and axitinib. The lung showed large areas of normal parenchyma (Figure 1 K) and only focal areas of thicker alveolar septae with inflammatory cells (Figure 1 J), compatible with moderate interstitial pneumonia. Interestingly, a complete anti-tumor response was also observed in mice treated with radiation and 5 weeks of axitinib when lung tissues were evaluated 5 weeks after discontinuation of axitinib (Table 2).

## Effect of axitinib and/or radiation on lung alveolar septa and evaluation of pneumonitis

To evaluate the effect of single and combined modalities on the lung architecture and determine whether the treatment induced pneumonitis at a late time point of 2 months after radiation and 5-10 weeks of treatment with axitinib, morphometric measurements of the thickness of alveolar septa were conducted on H&E stained lung tissue sections. The ratio of alveolar septa area relative to the total area of 20X field was quantified while contouring and excluding bronchi, bronchioles and large vessels (see inset Table 3). Data were stratified by using an arbitrary cut-off ratio of 0.3-0.49 for normal septa and 0.50-0.65 to define thick septa regarded as reflective of pneumonitis (see inset Table 3). Tumor-bearing lungs from control mice had a high percentage of areas with thickened septa of 60% compared to 20% in lungs from mice not bearing tumors (normal lung, Table 3). In multiple observations of slides from control tumors, these findings were consistent and suggested that the presence of tumor nodules causes pneumonitis, in agreement with the observations of focal areas of thick alveolar septa with hemorrhages surrounding tumor nodules (Figure 1B). The percent of thick septa areas in lungs treated with axitinib or radiation was lower (45%) than in control tumor bearing lungs that could be due to the much smaller tumor nodules in the lung tissue (Table 3). Following axitinib combined with radiation, the percent of thick septa was reduced to 30%, indicating a trend in decreasing pneumonitis by combining both modalities (Table 3). These quantitative data confirm our histology observations described above (Figure 1).

**Table 3.** Quantitation of alveolar septa thickness in lungs from mice treated with axitinib and radiation.

Ratio of Alveolar Septa Area/20X Field

| Treatment Area Ratio Range | Regular Septa[a] 0.3 - 0.49 Proportion | Percent | Thick Septa[b] 0.50 -0.65 Proportion | Percent | Regular Septa[c] 0.3 – 0.49 | Thick Septa[d] 0.50 – 0.65 |
|---|---|---|---|---|---|---|
| Tumor-Bearing Lungs | | | | | | |
| Control | 8/20 | 40% | 12/20 | 60% | | |
| Axitinib | 11/20 | 55% | 9/20 | 45% | | |
| Radiation | 11/20 | 55% | 9/20 | 45% |  |  |
| Rad + Ax (10w) | 14/20 | 70% | 6/20 | 30% | | |
| Rad + Ax (5w) | 14/20 | 70% | 6/20 | 30% | | |
| Normal Lung | 16/20 | 80% | 4/20 | 20% | | |

Using software analysis of H&E slides, the ratio of alveolar septa area relative to the total area of 20X field was quantified in 20 fields of 20X while contouring and excluding bronchioles and large vessels (see inset[c]). Data were stratified by using a ratio of 0.3-0.49 to define regular normal septa[a,c] and 0.50-0.65 to define thick septa[b,d] which is indicative of pneumonitis (see inset[d]). Data computed on lungs from 2 representative mice are presented.
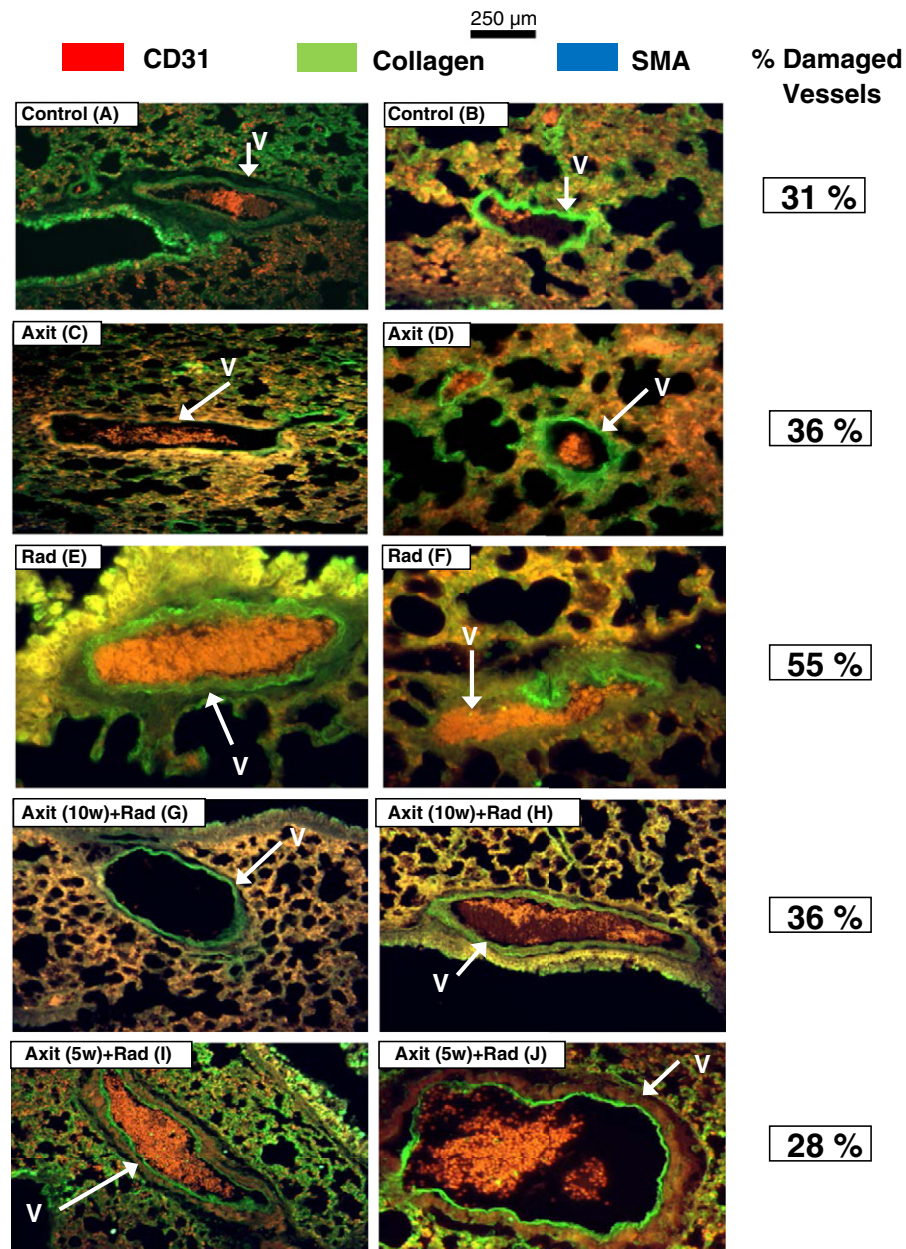
**Figure 2.** Fluorescent staining of vasculature in lung tissue sections from mice treated with axitinib and radiation. Lung tissue sections were immunostained with fluorescent dyes, including red for endothelial cells (anti-CD31), blue for pericytes (anti-SMA) and green for collagen (anti-collagen IV) as detailed in Materials & Methods. Representative images of large and small vessels (white arrows) of the lung tissues are presented. (A,B) Vessels with integral basement membranes from control mice. (C,D) Vessels from axitinib-treated mice showing disruptions or thickening in basement membrane collagen. (E,F) Vessels from radiation-treated mice showing thickening and projections or interruptions in the continuity of basement membrane collagen. Vessels with integral basement membranes are shown from mice treated with radiation and axitinib for up to 10 weeks (Axit + Rad in panels G,H) or in mice treated with radiation and axitinib for 5 weeks and then stopped (Axit (5w) + Rad in panels I,J). All 40X (bar size of 250 $\mu$m). The percentage of damaged vessels estimated in 20 fields of 40X, obtained from two mice per group, is reported in the third column.

## Effect of axitinib and/or radiation on lung vasculature

Lung tissue injury induced by radiotherapy leads to an inflammatory process caused by radiation damage to capillary endothelial cells and epithelial lung cells which results in pneumonitis and fibrosis. To assess further the effect of axitinib on the vasculature of the normal lung tissue, lung sections were stained with fluorescent anti-CD31 antibody, anti-SMA and anti-collagen to stain endothelial cells, pericytes and the vessel basement membranes, respectively. This fluorescent technique allows for visualization of vessel abnormalities including interruptions in the continuity of basement membrane collagen and/or thickening and projections in basement membrane, as previously described [34,35] Representative images of large and small vessels of the lung tissues are presented in Figure 2. We also quantitated the percent of damaged vessels in 20 fields of 40X. Vessels were considered damaged if the basement membrane was discontinuous (Figure 2C,F), or enlarged or had abnormal projections

(Figure 2E). Lungs from control mice showed a majority of vessels with integral basement membranes (Figure 2A,B), with 31% showing damage. Axitinib affected some of the vessels (about 36%) which showed interruptions in the basement membrane (Figure 2C) while other vessels had a full basement membrane (Figure 2D). Lungs treated with radiation showed alterations in the basement membrane of vessels including thickening and projections (Figure 2E) or interruptions in the continuity of the collagen (Figure 2 F), which occurred in 55% of the vessels, in agreement with our previous reported studies [32]. In lungs treated with axitinib combined with radiation a lower percentage of 36% vessels looked damaged while the other vessels looked healthy (Figure 2G,H). Stopping axitinib for the last 5 weeks of the experiment caused a decrease to 28% damaged vessels (Figure 2I,J). No significant difference was observed between the treatment groups but a trend in decreased damage in the lung vasculature was seen in axitinib + radiation compared to radiation alone (p = 0.13).
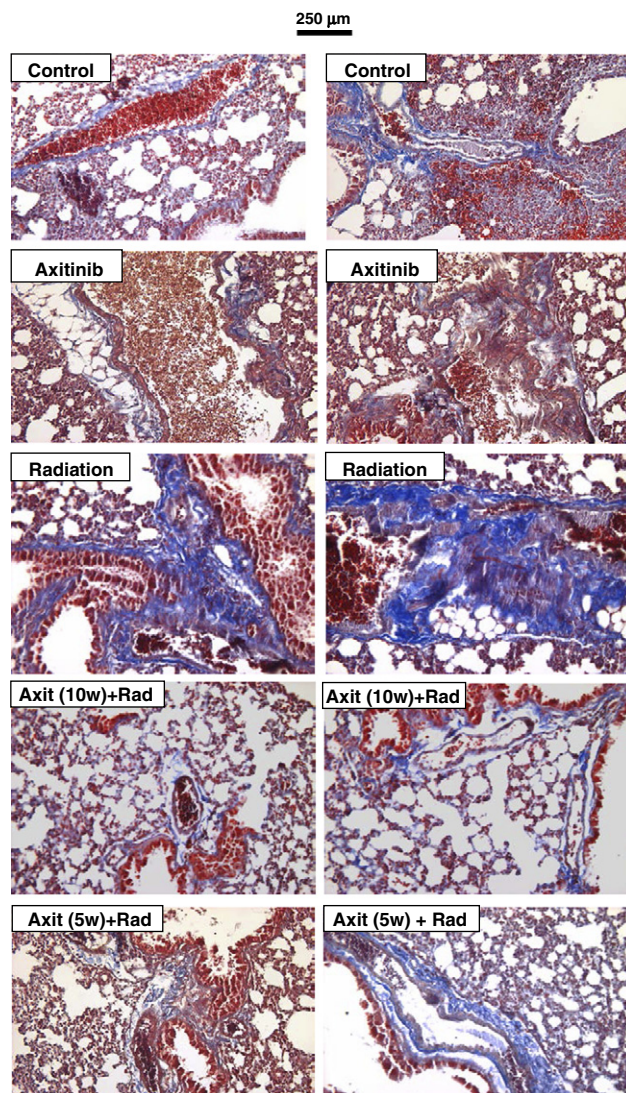
### Extent of fibrosis in lung tissue treated with axitinib and radiation

Lung pneumonitis induced by radiation is associated with fibrosis, which is a late event in radiation-induced injury and the result of an inflammatory process. The extent of fibrosis was evaluated in lung tissue sections using the Masson's Trichrome stain. At a late time point of over two months after radiation, we observed a dramatic increase in fibrosis in broncho-vascular bundles visualized by the intense blue staining of collagen fibers surrounding the vessels and bronchi (Figure 3, Table 2). These findings are typical of radiation induced damage in lung tissue and have been reproduced in several experiments in our laboratory. Increased fibrosis was not seen following axitinib treatment either alone or combined with radiation, the lung tissue was comparable to that of control mice (Figure 3,Table 2).

## Discussion

In an attempt to improve the therapeutic ratio of radiotherapy for inoperable Stage III locally advanced NSCLC, we have investigated the use of the anti-angiogenic drug axitinib to target the tumor vasculature given in conjunction with high dose irradiation of tumor-bearing lungs in the A549 xenograft NSCLC murine pre-clinical model.

In previous studies, we observed using DCE-MRI that pre-treatment of tumors for 3-4 days with the anti-angiogenic drug sunitinib regularizes the blood flow by trimming inefficient tumor vessels and potentiates radiotherapy of kidney tumors [28,29]. Therefore, mice bearing established lung tumors were pre-treated with axitinib for 4 days prior to lung irradiation, and then, axitinib treatment was continued after radiation. The endpoints for evaluation of the safety and therapeutic efficacy included assessing the duration of axitinib treatment, its effect on mouse weight and health in addition to the anti-tumor effect. Due to the anti-angiogenic property of axitinib, emphasis was put on analyzing the systemic effect of the drug on normal vasculature of the lungs and other organs to assess its specificity at targeting tumors. We found that daily administration of axitinib at 25 mg/kg for up to 3 months was well tolerated by the mice with a non-significant slight decrease in mouse weight which was reversed by discontinuation of axitinib. No other obvious signs of toxicity were observed during monitoring of the mice following axitinib given alone or in conjunction with lung irradiation.



**Figure 3.** Lung fibrosis in mice treated with axitinib and radiation. Lung tissue sections were stained with Masson's Trichrome to detect fibrosis. Bronchovascular bundles are shown in the lung tissues from control mice and mice treated with axitinib or radiation and both combined. Compared to thin collagen staining in lungs of control tumor-bearing mice (control), irradiated lungs (radiation) showed a drastic increase in fibrosis in broncho-vascular bundles, which is visualized as intense blue staining of collagen fibers surrounding the vessels and bronchioles. This finding was not seen mice treated with axitinib or with radiation combined with 10 weeks axitinib (Axit + Rad) or 5 weeks axitinib (Axit (5w) + Rad). All 40X (bar size of 250 μm).

Histological analysis of tissues from kidney, heart and liver showed that systemic treatment with axitinib did not cause disruption of vasculature in these tissues in contrast to our previous observations with sunitinib which did damage the vessels of kidneys [28]. These data suggest that long-term treatment with axitinib is safe and are in agreement with other pre-clinical studies in different tumor models [18,20,21]. In clinical trials, axitinib has demonstrated a predictable and manageable adverse event profile including diarrhea, hypertension, fatigue and nausea but no hematological or cardiovascular toxicity were reported [37,38].

Current trends in RT of NSCLC are exploring hypofractionation using higher doses per fraction with the total treatment given in a reduced number of fractions and less overall time, which is potentially more effective and more convenient to patients [39,40]. A high dose of lung irradiation combined with prolonged axitinib treatment was well tolerated and resulted in complete eradication of lung tumors in a stark contrast to the extensive invasion of lung tissue by large tumor nodules observed in control untreated mice. This dramatic therapeutic efficacy was observed histologically in the lungs of mice treated with axitinib for 10 weeks after radiation but also in lungs of mice in which axitinib was discontinued after five weeks, suggesting that this therapy does not require prolonged treatment. When given as single modalities, axitinib or radiation showed marked inhibition of tumor growth, decreasing tumor cellularity and proliferative rate as assessed Ki-67 marker. Either treatment also caused degenerative changes in the tumor cells and infiltration by inflammatory cells. However, the combination of a high single RT dose with axitinib was more effective than either single modality confirming potentiation of RT efficacy by axitinib. In long-term axitinib therapy after RT, we demonstrated a complete destruction of lung tumor nodules in the orthotopic lung model. Pre-clinical studies in subcutaneous prostate tumors demonstrated enhanced tumor response by combining axitinib and fractionated RT but these short term-studies of 2-3 weeks treatment documented tumor growth delays [20,21]. Normalization of vessel and blood flow did not seem to occur in these studies but they showed destruction of tumor vasculature. Other studies in different tumor models demonstrate a strong antigiogenic potential of axitinib by pruning tumor vessels and inducing tumor cell death observed by reduction of Ki-67 staining in agreement with the effect observed in our lung model [17,18].

In NSCLC patients treated with radiotherapy, radiation pneumonitis is an interstitial pulmonary inflammation that develops in up to 30% of patients [41,42]. It is caused by damage to lung parenchyma, epithelial cells, vascular endothelial cells and stroma that involves induction of pro-inflammatory cytokines and chemokines which recruit inflammatory immune cells in the lung tissue [43,44]. This acute early pneumonitis progresses to a chronic inflammation and culminates in the later stage of lung fibrosis which is due to excessive accumulation of collagen and other extracellular (ECM) components [31,44,45]. These adverse events of radiotherapy affect patients' breathing and their quality of life [41,42]. In the context of our current studies, there is concern that radiation-induced injury to lung tissue could be aggravated by vascular damage caused by anti-angiogenic treatment. To address this issue, the architecture and vasculature of lung tissues were investigated in the pre-clinical NSCLC model. Pneumonitis was quantified by measuring the thickness of alveolar septa [32]. In control tumor-bearing lungs, 60% thickened septa was observed and associated with inflammation and hemorrhages surrounding tumor nodules. This extensive pneumonitis can be attributed to the effect of the presence of large tumor nodules, at the late time points of 2-3 months and was also observed in other independent studies [32]. Lungs treated with either modality alone had both smaller tumor burden and less pneumonitis (45% thickened septa), suggesting a relation between tumor burden and pneumonitis. Pneumonitis was reduced to only 30% thickened septa in lungs treated with both RT and axitinib compared to 20% found in normal lungs. These findings taken together with the lack of residual tumor nodules suggest that axitinib given in conjunction with radiation may mitigate interstitial pneumonia that is caused by the presence of tumor and radiation.

The decreased pneumonitis observed by the combined therapy was further supported by histological staining and evaluation of vascular damage in the lung tissue. Pneumonitis has been associated with vascular damage induced by radiation. In the current and previous studies, we observed extensive hemorrhages induced by radiation [31]. Vascular damage plays an important role in the development of radiation-induced pulmonary toxicity and pulmonary hypertension. Fluorescent staining of the basement membrane of vessels showed that radiation caused alterations, interruptions and abnormal projections in the basement membrane of 55% of lung vessels whereas only 36% of vessels were altered in lungs treated with axitinib alone or combined with radiation compared to 31% in control lungs. Furthermore, stopping axitinib for the last 5 weeks of the experiment caused a decrease to 28% damaged vessels. These data suggest that axitinib causes moderate damage to normal lung vessels compared to RT and this effect is reversed by discontinuation of the drug. It is worth noting that axitinib did not exacerbate the damage caused by radiation to the normal vasculature of the lung and therefore axitinib may target more specifically tumor vessels.

Pneumonitis and fibrosis have been associated with lung injury induced by radiation. Radiation-induced pneumonitis and fibrosis were documented following single dose or fractionated radiation by 2-4 months after radiation in naïve mice and rats not-bearing lung tumors [46,47]. Our recently published studies in the A549 tumor model have shown that pneumonitis and fibrosis are detectable by 1 month after thoracic irradiation at a high dose of 10Gy or 12 Gy [31,32]. As pneumonitis induced by radiation becomes chronic, later time points of 2-4 months after lung irradiation showed both increased pneumonitis and fibrosis in naïve mice [33]. These studies suggest that radiation triggers a process of chronic inflammation with concurrent progressive development of fibrosis. In the current studies, at 2 months after radiation, prominent fibrosis was observed by increased collagen fibers supporting the vessel walls and bronchial walls which is in agreement with our previous studies. However, in lungs treated with radiation and axitinib, a striking decrease in fibrosis in lung tissue was observed. These data suggest that axitinib inhibits the formation of fibrosis induced by radiation. These intriguing results suggest a mechanism by which the anti-angiogenic drug could interfere with the inflammatory process induced by radiation. In the process of radiation-induced fibrogenesis, radiation activates the TGFβ signaling pathway, which is involved in epithelial-to-mesenchymal transition (EMT) leading to activation of fibroblasts and increased ECM and collagen deposition [44]. Axitinib acting as a receptor tyrosine kinase inhibitor could interfere with TGFβR and other growth factor receptors signaling involved in fibrogenesis to inhibit the cascade of events leading to fibroblast activation and fibrosis that is triggered by radiation [48]. Alternatively, axitinib may act like sunitinib and inhibit myeloid derived suppressor cells which could be involved in the inflammatory response caused by radiation [49]. Further studies are warranted to investigate these mechanisms.

Overall, our data demonstrate that axitinib is a potent and safe drug to use in conjunction with radiotherapy for lung cancer that could also act as a radioprotector for lung tissue by reducing pneumonitis and fibrosis.

# References

[1] Siegel R, Ma J, Zou Z, and Jemal A (2014). Cancer statistics. *CA Cancer J Clin* **64**, 9–29.

[2] van Meerbeeck JP, Meersschout S, De Pauw R, Madani I, and De Neve W (2008). Modern radiotherapy as part of combined modality treatment in locally advanced non-small cell lung cancer: present status and future prospects. *Oncologist* **13**, 700–708.

[3] Blackstock AW and Govindan R (2007). Definitive chemoradiation for the treatment of locally advanced non small-cell lung cancer. *J Clin Oncol* **25**, 4146–4152.

[4] Auperin A, Le Pechoux C, Rolland E, Curran WJ, Furuse K, Fournel P, Belderbos J, Clamon G, Ulutin HC, and Paulus R, et al (2010). Meta-analysis of concomitant versus sequential radiochemotherapy in locally advanced non-small-cell lung cancer. *J Clin Oncol* **28**, 2181–2190.

[5] Guida C, Maione P, Rossi A, Bareschino M, Schettino C, Barzaghi D, Elmo M, and Gridelli C (2008). Combined chemo-radiotherapy for locally advanced non-small cell lung cancer: current status and future development. *Crit Rev Oncol Hematol* **68**, 222–232.

[6] Ettinger DS (2010). Emerging profile of cetuximab in non-small cell lung cancer. *Lung Cancer* **68**, 332–337.

[7] Sandler A, Gray R, Perry MC, Brahmer J, Schiller JH, Dowlati A, Lilenbaum R, and Johnson DH (2006). Paclitaxel-carboplatin alone or with bevacizumab for non-small-cell lung cancer. *N Engl J Med* **355**, 2542–2550.

[8] Bonomi PD (2010). Implications of key trials in advanced nonsmall cell lung cancer. *Cancer* **116**, 1155–1164.

[9] Soria JC, Mauguen A, Reck M, Sandler AB, Saijo N, Johnson DH, Burcoveanu D, Fukuoka M, Besse B, and Pignon JP, et al (2013). Systematic review and meta-analysis of randomised, phase II/III trials adding bevacizumab to platinum-based chemotherapy as first-line treatment in patients with advanced non-small-cell lung cancer. *Ann Oncol* **24**, 20–30.

[10] Lind JS, Senan S, and Smit EF (2012). Pulmonary toxicity after bevacizumab and concurrent thoracic radiotherapy observed in a phase I study for inoperable stage III non-small-cell lung cancer. *J Clin Oncol* **30**, e104–e108.

[11] Socinski MA, Stinchcombe TE, Moore DT, Gettinger SN, Decker RH, Petty WJ, Blackstock AW, Schwartz G, Lankford S, and Khandani A, et al (2012). Incorporating bevacizumab and erlotinib in the combined-modality treatment of stage III non-small-cell lung cancer: results of a phase I/II trial. *J Clin Oncol* **30**, 3953–3959.

[12] Gomez DR, Gillin M, Liao Z, Wei C, Lin SH, Swanick C, Alvarado T, Komaki R, Cox JD, and Chang JY (2013). Phase 1 study of dose escalation in hypofractionated proton beam therapy for non-small cell lung cancer. *Int J Radiat Oncol Biol Phys* **86**, 665–670.

[13] Motzer RJ, Hutson TE, Tomczak P, Michaelson MD, Bukowski RM, Oudard S, Negrier S, Szczylik C, Pili R, and Bjarnason GA, et al (2009). Overall survival and updated results for sunitinib compared with interferon alfa in patients with metastatic renal cell carcinoma. *J Clin Oncol* **27**, 3584–3590.

[14] Socinski MA (2008). The current status and evolving role of sunitinib in non-small cell lung cancer. *J Thorac Oncol* **3**, S119–S123.

[15] Novello S, Scagliotti GV, Rosell R, Socinski MA, Brahmer J, Atkins J, Pallares C, Burgess R, Tye L, and Selaru P, et al (2009). Phase II study of continuous daily sunitinib dosing in patients with previously treated advanced non-small cell lung cancer. *Br J Cancer* **101**, 1543–1548.

[16] Kelly RJ and Rixe O (2009). Axitinib–a selective inhibitor of the vascular endothelial growth factor (VEGF) receptor. *Target Oncol* **4**, 297–305.

[17] Hu-Lowe DD, Zou HY, Grazzini ML, Hallin ME, Wickman GR, Amundson K, Chen JH, Rewolinski DA, Yamazaki S, and Wu EY, et al (2008). Nonclinical antiangiogenesis and antitumor activities of axitinib (AG-013736), an oral, potent, and selective inhibitor of vascular endothelial growth factor receptor tyrosine kinases 1, 2, 3. *Clin Cancer Res* **14**, 7272–7283.

[18] Ma J and Waxman DJ (2009). Dominant effect of antiangiogenesis in combination therapy involving cyclophosphamide and axitinib. *Clin Cancer Res* **15**, 578–588.

[19] Sennino B, Kuhnert F, Tabruyn SP, Mancuso MR, Hu-Lowe DD, Kuo CJ, and McDonald DM (2009). Cellular source and amount of vascular endothelial growth factor and platelet-derived growth factor in tumors determine response to angiogenesis inhibitors. *Cancer Res* **69**, 4527–4536.

[20] Fenton BM and Paoni SF (2007). The addition of AG-013736 to fractionated radiation improves tumor response without functionally normalizing the tumor vasculature. *Cancer Res* **67**, 9921–9928.

[21] Fenton BM and Paoni SF (2009). Alterations in daily sequencing of axitinib and fractionated radiotherapy do not affect tumor growth inhibition or pathophysiological response. *Radiat Res* **171**, 606–614.

[22] Schiller JH, Larson T, Ou SH, Limentani S, Sandler A, Vokes E, Kim S, Liau K, Bycott P, and Olszanski AJ, et al (2009). Efficacy and safety of axitinib in patients with advanced non-small-cell lung cancer: results from a phase II study. *J Clin Oncol* **27**, 3836–3841.

[23] Kozloff MF, Martin LP, Krzakowski M, Samuel TA, Rado TA, Arriola E, De Castro Carpeno J, Herbst RS, Tarazi J, and Kim S, et al (2012). Phase I trial of axitinib combined with platinum doublets in patients with advanced non-small cell lung cancer and other solid tumours. *Br J Cancer* **107**, 1277–1285.

[24] Horn L and Sandler A (2009). Epidermal growth factor receptor inhibitors and antiangiogenic agents for the treatment of non-small cell lung cancer. *Clin Cancer Res* **15**, 5040–5048.

[25] Scagliotti G and Govindan R (2010). Targeting angiogenesis with multitargeted tyrosine kinase inhibitors in the treatment of non-small-cell lung cancer. *Oncologist* **15**, 436–446.

[26] Salgia R (2011). Prognostic significance of angiogenesis and angiogenic growth factors in nonsmall cell lung cancer. *Cancer* **117**, 3889–3899.

[27] Aggarwal C, Somaiah N, and Simon G (2012). Antiangiogenic agents in the management of non-small cell lung cancer: where do we stand now and where are we headed? *Cancer Biol Ther* **13**, 247–263.

[28] Hillman GG, Singh-Gupta V, Zhang H, Al-Bashir AK, Katkuri Y, Li M, Yunker CK, Patel AD, Abrams J, and Haacke EM (2009). Dynamic contrast-enhanced magnetic resonance imaging of vascular changes induced by sunitinib in papillary renal cell carcinoma xenograft tumors. *Neoplasia* **11**, 910–920.

[29] Hillman GG, Singh-Gupta V, Al-Bashir AK, Yunker CK, Joiner MC, Sarkar FH, Abrams J, and Haacke EM (2011). Monitoring sunitinib-induced vascular effects to optimize radiotherapy combined with soy isoflavones in murine xenograft tumor. *Transl Oncol* **4**, 110–121.

[30] Hillman GG, Singh-Gupta V, Al-Bashir AK, Zhang H, Yunker CK, Patel AD, Sethi S, Abrams J, and Haacke EM (2010). Dynamic contrast-enhanced magnetic resonance imaging of sunitinib-induced vascular changes to schedule chemotherapy in renal cell carcinoma xenograft tumors. *Transl Oncol* **3**, 293–306.

[31] Hillman GG, Singh-Gupta V, Runyan L, Yunker CK, Rakowski JT, Sarkar FH, Miller S, Gadgeel SM, Sethi S, and Joiner MC, et al (2011). Soy isoflavones radiosensitize lung cancer while mitigating normal tissue injury. *Radiother Oncol* **101**, 329–336.

[32] Hillman GG, Singh-Gupta V, Hoogstra DJ, Abernathy L, Rakowski J, Yunker CK, Rothstein SE, Sarkar FH, Gadgeel S, Konski AA, Lonardo F, and Joiner MC (2013). Differential effect of soy isoflavones in enhancing high intensity radiotherapy and protecting lung tissue in a pre-clinical model of lung carcinoma. *Radiother Oncol* **109**, 117–125.

[33] Hillman GG, Singh-Gupta V, Lonardo F, Hoogstra DJ, Abernathy LM, Yunker CK, Rothstein SE, Rakowski J, Sarkar FH, and Gadgeel S, et al (2013). Radioprotection of Lung Tissue by Soy Isoflavones. *J Thorac Oncol* **8**, 1356–1364.

[34] Morikawa S, Baluk P, Kaidoh T, Haskell A, Jain RK, and McDonald DM (2002). Abnormalities in pericytes on blood vessels and endothelial sprouts in tumors. *Am J Pathol* **160**, 985–1000.

[35] Baluk P, Morikawa S, Haskell A, Mancuso M, and McDonald DM (2003). Abnormalities of basement membrane on blood vessels and endothelial sprouts in tumors. *Am J Pathol* **163**, 1801–1815.

[36] Bergers G and Song S (2005). The role of pericytes in blood-vessel formation and maintenance. *Neuro Oncol* **7**, 452–464.

[37] Bracarda S, Castellano D, Procopio G, Sepulveda JM, Sisani M, Verzoni E, and Schmidinger M (2014). Axitinib safety in metastatic renal cell carcinoma: suggestions for daily clinical practice based on case studies. *Expert Opin Drug Saf* **13**, 497–510.

[38] Gross-Goupil M, Francois L, Quivy A, and Ravaud A (2013). Axitinib: A Review of its Safety and Efficacy in the Treatment of Adults with Advanced Renal Cell Carcinoma. *Clin Med Insights Oncol* **7**, 269–277.

[39] Senan S, Palma DA, and Lagerwaard FJ (2011). Stereotactic ablative radiotherapy for stage I NSCLC: Recent advances and controversies. *J Thorac Dis* **3**, 189–196.

[40] Timmerman R, Paulus R, Galvin J, Michalski J, Straube W, Bradley J, Fakiris A, Bezjak A, Videtic G, and Johnstone D, et al (2010). Stereotactic body radiation therapy for inoperable early stage lung cancer. *JAMA* **303**, 1070–1076.

[41] Kong FM, Hayman JA, Griffith KA, Kalemkerian GP, Arenberg D, Lyons S, Turrisi A, Lichter A, Fraass B, and Eisbruch A, et al (2006). Final toxicity results of a radiation-dose escalation study in patients with non-small-cell lung cancer

(NSCLC): predictors for radiation pneumonitis and fibrosis. *Int J Radiat Oncol Biol Phys* **65**, 1075–1086.

[42] Jin H, Tucker SL, Liu HH, Wei X, Yom SS, Wang S, Komaki R, Chen Y, Martel MK, and Mohan R, et al (2009). Dose-volume thresholds and smoking status for the risk of treatment-related pneumonitis in inoperable non-small cell lung cancer treated with definitive radiotherapy. *Radiother Oncol* **91**, 427–432.

[43] Hill RP (2005). Radiation effects on the respiratory system. *BJR Suppl* **27**, 75–81.

[44] Bentzen SM (2006). Preventing or reducing late side effects of radiation therapy: radiobiology meets molecular pathology. *Nat Rev Cancer* **6**, 702–713.

[45] Yarnold J and Brotons MC (2010). Pathogenetic mechanisms in radiation fibrosis. *Radiother Oncol* **97**, 149–161.

[46] Calveley VL, Jelveh S, Langan A, Mahmood J, Yeung IW, Van Dyk J, and Hill RP (2010). Genistein can mitigate the effect of radiation on rat lung tissue. *Radiat Res* **173**, 602–611.

[47] Para AE, Bezjak A, Yeung IW, Van Dyk J, and Hill RP (2009). Effects of genistein following fractionated lung irradiation in mice. *Radiother Oncol* **92**, 500–510.

[48] Kalluri R and Zeisberg M (2006). Fibroblasts in cancer. *Nat Rev Cancer* **6**, 392–401.

[49] Ko JS, Zea AH, Rini BI, Ireland JL, Elson P, Cohen P, Golshayan A, Rayman PA, Wood L, and Garcia J, et al (2009). Sunitinib mediates reversal of myeloid-derived suppressor cell accumulation in renal cell carcinoma patients. *Clin Cancer Res* **15**, 2148–2157.